Tools for large-eddy simulation

By David A. Caughey † AND Giridhar Jothiprasad †

A computer code has been developed for solving the incompressible Navier-Stokes equations for test flows that will allow the comparison of various strategies for assessing the accuracy of LES solutions for flows at large Reynolds number, where it is impractical to make direct comparisons with DNS solutions for the same flow. The code includes options for a conventional Smagorinsky subgrid model, as well as hyperviscosity dissipative terms that will allow a greater separation of scales for high Reynolds number flows. In this report, the code is validated for several simple, periodic flows, including the Taylor-Green vortex and decaying isotropic turbulence, and preliminary results are presented, showing good agreement for (forced, periodic) Kolmogorov flow in the limit of high Reynolds number, on relatively modest meshes using the hyperviscosity dissipation.

1. Introduction

Large Eddy Simulation (LES) holds the promise of improved prediction of turbulent flows at large Reynolds numbers relative to computations using the Reynolds-averaged equations, with substantially less computational cost than that required for Direct Numerical Simulation (DNS) since only the largest, most energetic, scales need to be resolved. Nevertheless, the computational resources required for LES computations for all but the simplest flows remain substantial. The required resources are so great, in fact, that most LES computations are performed at the limits of available resources, and it usually is not clear to what extent the solutions are resolved. Furthermore, since the accuracy of the computation is not assessed in any systematic way, the most frequently used metric for the performance of LES is comparison with DNS computations which, as a result of the computational resources required for DNS, necessarily limits these assessments to flows at relatively low Reynolds numbers.

In order for LES to become useful for practical engineering problems, tools must be developed that allow one to estimate the accuracy of the LES solution without having to make a direct comparison with a DNS solution for the same flow. The availability of such tools would free one from the need to make comparisons only at low Reynolds numbers where DNS solutions are feasible, and permit the evaluation of LES at the larger Reynolds numbers for which LES is most attractive, and where the separation between the energetic and dissipative scales is large enough that the LES approach has some theoretical basis.

The long-term objective of the authors' work is to develop tools suitable for assessing the accuracy of LES solutions, especially for flows at large Reynolds number. As a first step in this process, the authors have developed a computer code for solving the incompressible Navier-Stokes equations, including additional hyperviscosity dissipation, for test flows that will allow the comparison of various accuracy-assessment strategies. The incorporation of hyperviscosity dissipation (based on the biharmonic of the velocity field) is motivated by the desire to increase the separation of the energetic and dissipative

† Cornell University

scales, so that the high Reynolds number limit of solutions can be studied on meshes of relatively modest resolution.

In this report, validations of the code are presented for several simple, periodic flows, including the Taylor-Green vortex and decaying, isotropic turbulence, and preliminary results show good agreement for (forced, periodic) Kolmogorov flow in the limit of high Reynolds number, on relatively modest meshes using the hyperviscosity dissipation.

2. Algorithm

In this section we describe a variant of the fractional-step method (Chorin (1968), Temam (1969), Kim & Moin (1985)) used for the time-advancement of the incompressible Navier-Stokes equations with a Smagorinsky model and added hyperviscosity dissipation.

The constant-density Navier-Stokes equations, with an added hyperviscosity, and the continuity equation

$$\frac{\partial u_i}{\partial t} + \frac{\partial \left(u_i u_j\right)}{\partial x_j} = -\frac{\partial p}{\partial x_i} + \left(\nu + \nu_r\right) \frac{\partial^2 u_i}{\partial x_j \partial x_j} + \nu_4 \frac{\partial^4 u_i}{\partial x_j \partial x_j \partial x_l \partial x_l} \tag{2.1}$$

$$\frac{\partial u_i}{\partial x_i} = 0 \tag{2.2}$$

are discretized on a staggered grid. Velocities u_i are defined at the centers of cell faces having normals in the direction x_i, and the pressure is defined at the cell center. The equations are marched in time using an explicit approximation for the convective terms and an iterative Alternating Direction Implicit (ADI) scheme for the viscous (and hyperviscous) terms. Such a fractional-step time-advancement scheme for (2.1) and (2.2) can be written as

$$\begin{aligned} \frac{\hat{u}_i - u_i^n}{\Delta t} + \left[\frac{3}{2} H_i\left\{\mathbf{u^n}\right\} - \frac{1}{2} H_i\left\{\mathbf{u^{n-1}}\right\}\right] + G_i\left\{\phi^n\right\} = \\ \frac{\nu + \nu_r}{2}\left[D_2\left\{\hat{u}_i\right\} + D_2\left\{u_i^n\right\}\right] + \frac{\nu_4}{2}\left[D_4\left\{\hat{u}_i\right\} + D_4\left\{u_i^n\right\}\right] \end{aligned} \tag{2.3}$$

$$\frac{u_i^{n+1} - \hat{u}_i}{\Delta t} = -G_i\left\{\delta\phi^{n+1}\right\}, \tag{2.4}$$

with

$$C\left\{\mathbf{u^{n+1}}\right\} = 0 \tag{2.5}$$

$$\phi^{n+1} = \phi^n + \delta\phi^{n+1} \tag{2.6}$$

where

$$H_i\left\{\mathbf{u}\right\} \equiv \text{Spatial discretization of } \frac{\partial \left(u_i u_j\right)}{\partial x_j}$$

$$G_i\left\{\phi\right\} \equiv \text{Spatial discretization of } \frac{\partial \phi}{\partial x_i}$$

$$D_2\left\{u_i\right\} \equiv \text{Spatial discretization of } \frac{\partial^2 u_i}{\partial x_j \partial x_j}$$

$$D_4\left\{u_i\right\} \equiv \text{Spatial discretization of } \frac{\partial^4 u_i}{\partial x_j \partial x_j \partial x_l \partial x_l}$$

$$C\left\{\mathbf{u}\right\} \equiv \text{Spatial discretization of } \frac{\partial u_i}{\partial x_i}.$$

The convective terms $H_i\{\}$ are discretized to fourth-order spatial accuracy using central differences, and the time advancement is carried out using a second-order Adams-Bashforth approximation for the convective terms. The spatial discretization of the convective terms is designed to be energy conserving (Morinishi & Moin (1998)) in order to achieve explicit control over the dissipation introduced in the numerical scheme. The viscous diffusion terms $D_2\{\}$ are discretized to fourth order spatial accuracy, while the hyperviscous terms $D_4\{\}$ are discretized to second order spatial accuracy, both using central differences. These two terms are advanced in time using an iterative ADI scheme. It should be noted that ϕ differs from the pressure by an $O(\Delta t)$ term (Kim & Moin (1985)).

The scheme has been implemented for periodic boundary conditions on a uniform grid. Equation (2.5) can be used to eliminate u_i^{n+1} from the divergence of (2.4), giving a Poisson equation for $\delta\phi^{n+1}$

$$C\left\{\mathbf{G}\left\{\delta\phi^{n+1}\right\}\right\} = -\frac{C\{\hat{\mathbf{u}}\}}{\Delta t} \tag{2.7}$$

Further details of the spatial discretization can be found in Morinishi & Moin (1998).

The implicit equations arising at each time step are solved using an iterative ADI scheme. We first define a splitting of the operators $D_2\{\}$ and $D_4\{\}$ into differences in the x_1, x_2 and x_3 directions and cross derivatives as follows,

$$\begin{aligned}
D_2\{u_i\} &= D_{2_{x_1}}\{u_i\} + D_{2_{x_2}}\{u_i\} + D_{2_{x_3}}\{u_i\} \\
D_{2_{x_j}}\{u_i\} &\equiv \text{Spatial discretization of } \frac{\partial^2 u_i}{\partial x_j^2} \\
D_4\{u_i\} &= D_{4_{x_1}}\{u_i\} + D_{4_{x_2}}\{u_i\} + D_{4_{x_3}}\{u_i\} + D_{4_{\text{cross}}}\{u_i\} \\
D_{4_{x_j}}\{u_i\} &\equiv \text{Spatial discretization of } \frac{\partial^4 u_i}{\partial x_j^4} \\
D_{4_{\text{cross}}}\{u_i\} &\equiv \text{Spatial discretization of } 2\left[\frac{\partial^4 u_i}{\partial x_1^2 \partial x_2^2} + \frac{\partial^4 u_i}{\partial x_2^2 \partial x_3^2} + \frac{\partial^4 u_i}{\partial x_3^2 \partial x_1^2}\right].
\end{aligned}$$

Let $\hat{u}_i^{[m]}$ denote the approximation to $\hat{u}_i$ at the m^{th} iteration. Equation (2.3) can be rewritten as

$$\begin{aligned}
\frac{\hat{u}_i^{[m+1]}}{\Delta t} + \left\langle \frac{-u_i^n}{\Delta t} \right\rangle = &\left\langle \frac{3}{2} H_i\{\mathbf{u^n}\} - \frac{1}{2} H_i\left\{\mathbf{u^{n-1}}\right\} - G_i\{\phi^n\} \right\rangle + \\
&\frac{\nu+\nu_r}{2} D_2\left\{\hat{u}_i^{[m+1]}\right\} + \left\langle \frac{\nu+\nu_r}{2} D_2\{u_i^n\} \right\rangle + \\
&\frac{\nu_4}{2}\left[D_{4_{x_1}}\left\{\hat{u}_i^{[m+1]}\right\} + D_{4_{x_2}}\left\{\hat{u}_i^{[m+1]}\right\} + D_{4_{x_3}}\left\{\hat{u}_i^{[m+1]}\right\}\right] + \\
&\frac{\nu_4}{2} D_{4_{\text{cross}}}\left\{\hat{u}_i^{[m]}\right\} + \left\langle \frac{\nu_4}{2} D_4\{u_i^n\} \right\rangle
\end{aligned} \tag{2.8}$$

The terms within angle braces do not change with iteration m, and can be grouped

together to form the source term

$$S_i\left\{\mathbf{u^n},\mathbf{u^{n-1}}\right\} \equiv \frac{u_i^n}{\Delta t} + \frac{3}{2}H_i\left\{\mathbf{u^n}\right\} - \frac{1}{2}H_i\left\{\mathbf{u^{n-1}}\right\} - G_i\left\{\phi^n\right\} + \frac{\nu+\nu_r}{2}D_2\left\{u_i^n\right\} + \frac{\nu_4}{2}D_4\left\{u_i^n\right\} \tag{2.9}$$

Equation 2.8 then reduces to

$$\left(\frac{1}{\Delta t} - \frac{\nu+\nu_r}{2}\left[D_{2_{x_1}} + D_{2_{x_2}} + D_{2_{x_3}}\right] - \frac{\nu_4}{2}\left[D_{4_{x_1}} + D_{4_{x_2}} + D_{4_{x_3}}\right]\right)\left\{\hat{u}_i^{[m+1]} - \hat{u}_i^{[m]}\right\} \tag{2.10}$$

$$\begin{aligned} &= S_i\left\{\mathbf{u^n},\mathbf{u^{n-1}}\right\} + \frac{-\hat{u}_i^{[m]}}{\Delta t} + \frac{\nu+\nu_r}{2}D_2\left\{\hat{u}_i^{[m]}\right\} + \frac{\nu_4}{2}D_4\left\{\hat{u}_i^{[m]}\right\} \\ &\equiv R_i\left\{\hat{u}_i^{[m]},\mathbf{u^n},\mathbf{u^{n-1}}\right\} \end{aligned}$$

It is easily seen that the right-hand side of (2.10) is simply the residual evaluated at $\hat{u}_i^{[m]}$. Multiplying (2.10) by Δt and approximating the left-hand side using ADI gives

$$\begin{aligned} &\left(1 - \frac{\Delta t}{2}\left[(\nu+\nu_r)\,D_{2_{x_1}} + \nu_4 D_{4_{x_1}}\right]\right)\left(1 - \frac{\Delta t}{2}\left[(\nu+\nu_r)\,D_{2_{x_2}} + \nu_4 D_{4_{x_2}}\right]\right)\cdot \\ &\left(1 - \frac{\Delta t}{2}\left[(\nu+\nu_r)\,D_{2_{x_3}} + \nu_4 D_{4_{x_3}}\right]\right)\left\{\hat{u}_i^{[m+1]} - \hat{u}_i^{[m]}\right\} = \Delta t R_i\left\{\hat{u}_i^{[m]},\mathbf{u^n},\mathbf{u^{n-1}}\right\} \end{aligned} \tag{2.11}$$

Equation (2.11) requires inversions only of tridiagonal matrices, as opposed to the large sparse matrices required in (2.10). When the coefficients ν_r and ν_4 vary spatially, the left-hand side of Eq. 2.11 is further approximated by replacing the coefficients with their corresponding spatial averages, while the right-hand side is computed exactly. It has been found by numerical experimentation that three iterations are usually sufficient to reduce the residual by at least four orders of magnitude.

3. Results

Here we present results of several flows to validate the computer code described in the preceding section, and preliminary results to show its promise for computing flows at high Reynolds number. All flows considered here are periodic and are solved in a three-dimensional periodic box of edge size 2π.

3.1. *Code validation*

The periodic two-dimensional vortex problem was used extensively to validate the spatial and temporal accuracy of the code. The initial conditions for a periodic vortical flow in the x_1-x_2 plane are given by

$$\begin{aligned} u_1 &= -\cos x_1 \sin x_2\,, \\ u_2 &= \cos x_2 \sin x_1\,, \\ u_3 &= 0\,. \end{aligned} \tag{3.1}$$

The numerical solutions obtained are compared with the known analytical solutions. In order to completely validate the difference coding for all 3 directions, solutions for a

periodic vortex in the x_2–x_3 plane also were computed. Although the test problem has some symmetries, any serious error in the code could have been detected using this test case.

Mesh refinement studies were used to verify the spatial order of accuracy, which was confirmed to be fourth-order for the Navier-Stokes equations (i.e., without the hyperviscosity dissipation) and second order when the hyperviscosity terms are included. Similarly, the temporal order of accuracy was verified to be second order.

3.2. *Taylor-Green Vortex*

Next, the code was used to carry out a DNS of the Taylor-Green vortex flow (Brachet et al. (1983)). This flow is one of the simplest systems in which one can study the generation of small scales and the turbulence resulting from three-dimensional vortex stretching. The initial conditions for the Taylor-Green vortex flow are

$$\begin{aligned} u_1 &= \frac{2}{\sqrt{3}} \sin\left(\frac{2\pi}{3}\right) \sin x_1 \cos x_2 \cos x_3 \,, \\ u_2 &= -\frac{2}{\sqrt{3}} \sin\left(\frac{2\pi}{3}\right) \cos x_1 \sin x_2 \cos x_3 \,, \\ u_3 &= 0 \,. \end{aligned} \tag{3.2}$$

The Reynolds number for this flow is defined as $\mathbf{Re} \equiv 1/\nu$. The DNS of the Taylor-Green flow was carried out on a 64^3 mesh for $\mathbf{Re} = 100$, 200, 300 and 400. Since the smallest scales generated in the $\mathbf{Re} = 400$ simulation were not resolved on this mesh, the DNS was repeated on a 128^3 mesh. All computations were performed at a constant Courant number $\mathcal{C} = 0.5$.

The time histories of the dissipation rate are compared with results of the fully-resolved spectral computations of Jeanmart (2002) in figure 1. The figure shows that the time history of the dissipation rate is well predicted in our 64^3 simulations for the lower Reynolds numbers, but that there are discrepancies between the present results on the 64^3 mesh and the reference computations in the vicinity of the maximum dissipation for the computation at $\mathbf{Re} = 400$; however, the present results agree well with the reference computation when repeated on the 128^3 mesh.

3.3. *Decaying, isotropic turbulence*

The case of decaying, isotropic turbulence allows comparison of results computed with various subgrid-scale models to those of fully-resolved DNS computations for modest Reynolds numbers. Two different subgrid-scale models were compared:

(*a*) *Smagorinsky model*: An eddy-viscosity model of the form,

$$\nu_r = (C_r \Delta)^2 \left(S_{ij} S_{ij}\right)^{\frac{1}{2}} \tag{3.3}$$

where S_{ij} is the local rate-of-strain tensor, Δ is the mesh spacing, and the Smagorinsky coefficient is taken to be $C_r = 0.17$, following Lilly's analysis (Lilly (1967)).

(*b*) *Smagorinsky-type hyperviscosity model*: A hyperviscosity model of the form,

$$\nu_4 = (C_4 \Delta)^4 \left(S_{ij} S_{ij}\right)^{\frac{1}{2}} \tag{3.4}$$

where S_{ij} is the again the local rate-of-strain tensor, Δ is the mesh spacing, and the (dimensionless) constant $C_4 \approx 0.278$ is chosen such that the flow is fully resolved on the given grid. (Note: it is clear from Eq. (2.1) that the dimensions of ν_4 are length^4/time.)

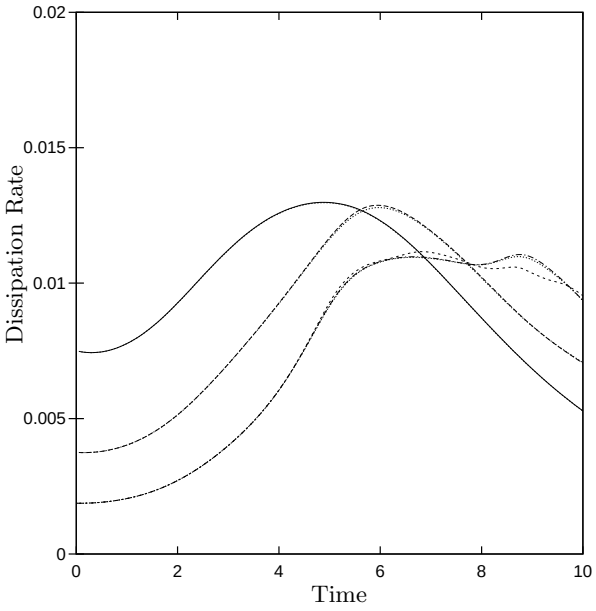

FIGURE 1. History of dissipation rate for Taylor-Green flow at various Reynolds numbers. **Re** = 100: solid line; **Re** = 200: broken line; **Re** = 400: 64^3 grid is dashed line, 128^3 grid is dash-dotted line. Comparison with spectral computations of Jeanmart, shown as dotted lines; dotted lines are invisible when overplotted with current results.

Large-eddy simulations (LES) of decaying, isotropic turbulence were performed on a 64^3 grid using both these models. An under-resolved DNS was also carried out on the 64^3 mesh. The initial conditions were provided by Alan Wray from a 256^3 spectral simulation of forced, isotropic turbulence (Wray 2002). The initial spectral field was first truncated to 64^3 spectral modes and then appropriately transformed to physical space to be used as initial conditions on the 64^3 staggered mesh. The results of the LES were compared with a direct spectral simulation for decaying turbulence carried out by Wray with the full 256^3 spectral modes, using the same initial condition. Figure 2 compares the time history of the turbulence kinetic energy for the various computations. For the purposes of this comparison, only the kinetic energy in the first 64^3 modes of Wray's full DNS are plotted. The figure shows that the results obtained using the Smagorinsky-type hyperviscosity model agree best with results of the full 256^3 simulation.

Figure 3 compares the energy spectra from the three different computations at a relatively early time in the computations. It is seen that in the case where there was no subgrid-scale model there is an accumulation of energy at the higher wavenumbers, since the physical viscosity is unable to remove energy from the small scales at a sufficiently fast rate. It is also seen that the two computations using subgrid-scale models were well resolved on the 64^3 mesh.

3.4. *Kolmogorov flow*

Kolmogorov flow is an open flow in a periodic box, driven by a large-scale steady forcing in the x_1-direction given by,

$$f_1 = -F \sin(\kappa_f x_2); \qquad \kappa_f = 1; \qquad F = 0.16 \tag{3.5}$$

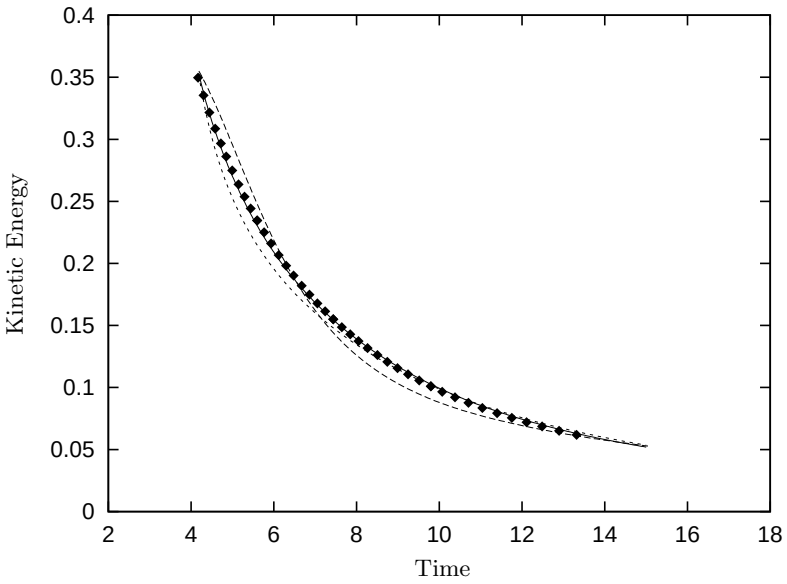

FIGURE 2. History of the kinetic energy decay for isotropic turbulence. LES computation using: no subgrid model (dotted line); Smagorinsky model (dashed line); and Smagorinsky type hyperviscosity model (solid line) carried out on a 64^3 grid. Reference DNS computation by Wray using 256^3 spectral modes (⧫).

The high-Reynolds-number limit of this flow has been studied by Borue & Orszag (1996) and Shebalin & Woodruff (1997). Breaking of the symmetries imposed by the forcing has been studied by Jeanmart, Carati & Wincklemans (2002) (2002) in computations using box sizes larger than the period of the forcing.

In order effectively to increase the extent of the inertial range, we use only hyperviscous dissipation. Since the Kolmogorov flow is characterized by the amplitude of the force F, the spatial frequency of the forcing function κ_f, and the hyperviscosity ν_4, we define the following velocity and time scales and a Reynolds number based on the hyperviscosity (Borue & Orszag (1996)).

$$U_0 = 2.5\left(\frac{F}{\kappa_f}\right)^{0.5} \tag{3.6}$$

$$t_0 = \frac{1}{(F\kappa_f)^{0.5}} \tag{3.7}$$

$$\mathbf{Re} = \frac{U_0}{\kappa_f^3 \nu_4} \tag{3.8}$$

This flow is a good test case for the following reasons:

(a) The flow has a statistically stationary state.

(b) The flow is believed to have a well-defined high Reynolds number limit (Borue & Orszag (1996)), for which the turbulent intensities, energy dissipation rates, and various terms in the energy balance equations have a simple coordinate dependence, $a+b\cos 2x_2$. This makes Kolmogorov flow a good model to explore the applicability of turbulent transport approximations in open flows.

(c) Since the sinusoidal forcing has only one spatial frequency ($\kappa_f = 1$) and a constant

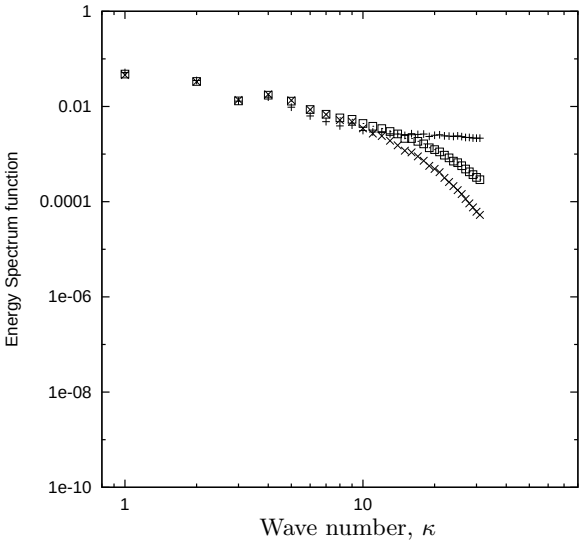

FIGURE 3. Comparison of the instantaneous energy spectra from the computations using: only molecular viscosity (+), molecular viscosity plus the Smagorinsky model (×), and molecular viscosity plus the Smagorinsky-like hyperviscosity model (□), at very early times.

amplitude F, the exact amount of energy input into the large scale can be calculated. At a sufficiently high Reynolds number, when a statistically steady state is reached, the amount of energy input into the large scales is equal to the amount of energy dissipated ϵ. This is one of the flows in which ϵ can be estimated exactly and hence enables us to estimate other length and velocity scales more accurately.

(*d*) The boundary conditions are periodic in all three directions, which means that the existing DNS code could be easily modified to include the sinusoidal forcing.
While this flow has been studied extensively using DNS, generating such a flow in the laboratory would be difficult. However, the flow in the vicinity of the inflection points of the mean profile should be similar to that for homogeneous shear flow.

In the present LES computations, the flow was initialized to the solution of an analogous laminar flow problem plus an added isotropic velocity fluctuation. The fluctuations were found to eliminate the otherwise long transient time needed for the turbulent fluctuations to develop and grow. The flow properties were averaged over planes containing the statistically-homogeneous directions (x_1 and x_3), and over time using a variant of moving averages. It was found necessary to average the flow quantities over a large number of eddy turnover times to obtain statistically reliable profiles of mean velocity, velocity autocorrelations, and Reynolds stress. The time averaging was begun only after the flow had reached a statistically-stationary state. It has been observed by Borue & Orszag (1996) that the statistically stationary state has a mean velocity profile that becomes independent of the Reynolds number for sufficiently large values of Reynolds number. The present simulations were carried out on both 64^3 and 32^3 grids. Figure 4 show the time history of turbulence kinetic energy and dissipation rate, while figure 5 shows the instantaneous energy spectra for the flow using hyperviscosity computations on the 64^3 grid. Figure 6 compares the mean velocity and velocity correlations obtained from the 64^3 hyperviscosity computation with the analytical curves found by Borue & Orszag

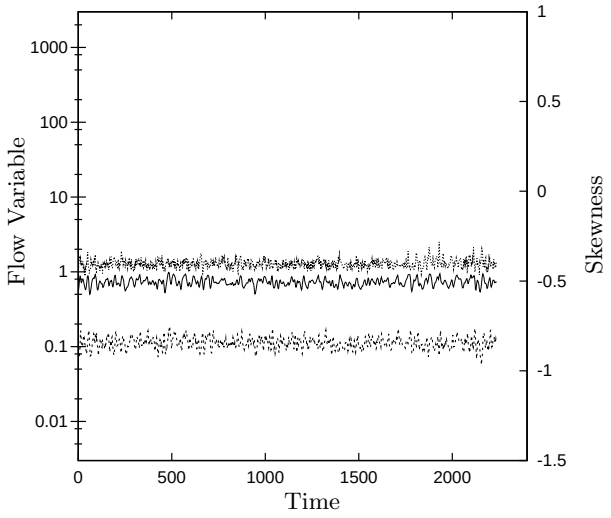

FIGURE 4. Time history of development of mean quantities for the Kolmogorov flow hyperviscosity computations on a 64^3 grid. Upper curve is skewness, middle curve is average energy, and lower curve is dissipation rate.

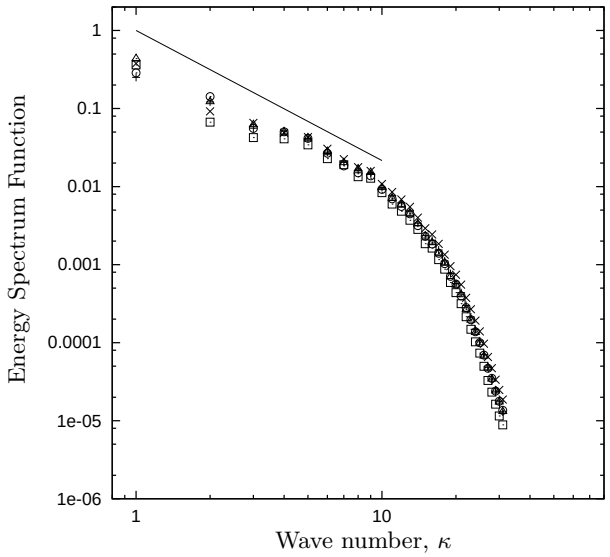

FIGURE 5. Instantaneous mean energy spectra for the Kolmogorov flow hyperviscosity computations on a 64^3 grid. Spectra are plotted at times $t = 2071$ (+), 2089 ($\times$), 2107 ($\odot$), 2124 ($\boxdot$), and 2143 ($\triangle$).

(1996) to fit the high Reynolds number limit. The agreement is quite good in spite of the relative coarseness of the grid used here.

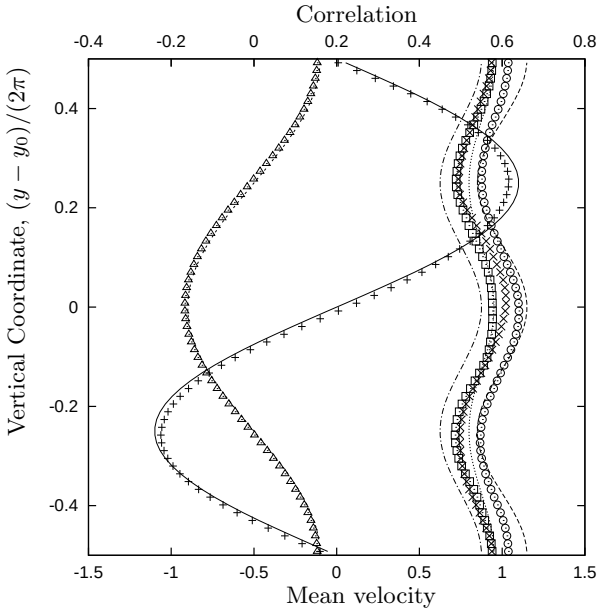

FIGURE 6. Mean velocity and velocity correlations for Kolmogorov flow; symbols are results from hyperviscosity computations on a 64^3 grid with $\nu_4 = 0.006$, and lines are high-Reynolds-number curve fits by Borue & Orszag (1996). Variables plotted are: $\langle u_1 \rangle$, + and solid line; $\langle u_1 u_2 \rangle$, $\triangle$ and short dashed line; $\langle u_1 u_1 \rangle$, $\times$ and long dashed line; $\langle u_2 u_2 \rangle$, $\odot$ and dotted line; $\langle u_3 u_3 \rangle$, $\boxdot$ and dash-dot line.

4. Conclusions

As a first step in developing tools suitable for assessing the accuracy of LES solutions for flows at large Reynolds number, the authors have developed a computer code for solving the incompressible Navier-Stokes equations for test flows that will allow the comparison of various accuracy-assessment strategies. The code includes a conventional Smagorinsky sub-grid model, as well as hyperviscosity dissipative terms that will allow greater separation of the energy-containing and dissipative scales for high Reynolds number flows. The code is validated for several simple, periodic flows, including the Taylor-Green vortex and decaying, isotropic turbulence, and preliminary results show good agreement with the high Reynolds number limit for (forced, periodic) Kolmogorov flow on relatively modest meshes using the hyperviscosity dissipation. The benefits of using the Kolmogorov flow for these studies are described, and future results will concentrate on comparisons of methods for accurately predicting the statistics of the energetic scales for this flow.

REFERENCES

BORUE, V. & ORSZAG, S. A. 1996 Numerical study of three-dimensional Kolmogorov flow at high Reynolds numbers. *J. Fluid Mech.* **306**, 293-323.

BRACHET, M. E., MEIRON, D. I., ORSZAG, S. A., NICKEL, B. G., MORF, R. H. & FRISCH, U. 1983 Small-scale structure of the Taylor-Green vortex. *J. Fluid Mech.* **130**, 411-452.

Chorin, A. J. 1968 Numerical solution of the Navier-Stokes equations. *Math. Comput.* **22**, 745-762.

Jeanmart, H. 2002 Private communication. *Centre for Systems Engineering and Applied Mechanics, Université Catholique de Louvain, 1348 Louvain-la-Neuve, Belgium*. Note: The (unpublished) results provided by Jeanmart are equivalent to those plotted in figure 7 of Brachet et al. (1983).

Jeanmart, H., Carati, D. & Winckelmans, G. S. 2002 Non universality and symmetry breaking in three-dimensional turbulent Kolmogorov flow. Submitted to *Phys. Fluids*.

Kim, J. & Moin, P. 1985 Application of a fractional-step method to incompressible Navier-Stokes equations. *J. Comput. Phys.* **59**, 308-323.

Lilly, D. K. 1967 The representation of small-scale turbulence in numerical simulation experiments. *Proc. IBM Scientific Computing Symposium on Environmental Sciences* IBM Form No. **320-1951**, 195-210.

Morinishi, Y., Lund, T. S., Vasilyev, O. V. & Moin, P. 1998 Fully conservative higher order finite difference schemes for incompressible flow. *J. Comput. Phys.* **143**, 90-124.

Shebalin, J. V. & Woodruff, S. L. 1997 Kolmogorov flow in three dimensions. *Phys. Fluids*, **9**, 164-170.

Temam, R. 1969 Sur l'approximation de la solution des equations de Navier-Stokes par la méthode des pas fractionnaires. *Arch. Rational Mech. Anal.* **32**, 135-153 and **33**, 377-385.

Wray, A. 2002 Private communication. *NASA Ames Research Center.*